Inorganic Chemistry

Article

pubs.acs.org/IC

Synthesis and Solid-State Structural Characterization of a Series of Aqueous Heterometallic Tridecameric Group 13 Clusters

Maisha K. Kamunde-Devonish,[†] Dylan B. Fast,[§] Zachary L. Mensinger,[†,⊥] Jason T. Gatlin,[†] Lev N. Zakharov,[‡] Michelle R. Dolgos,*[,§] and Darren W. Johnson*[,†]

[†]Department of Chemistry & Biochemistry and the Materials Science Institute and [‡]Center for Advanced Materials Characterization in Oregon (CAMCOR), University of Oregon, Eugene, Oregon 97403-1253, United States

[§]Department of Chemistry, Oregon State University, 153 Gilbert Hall, Corvallis, Oregon 97331-4003, United States

Supporting Information

ABSTRACT: The synthesis and solid-state characterization of a complete series of new heterometallic aqueous nanoscale Ga/In tridecameric clusters is presented. These hydroxo−aquo species significantly expand the library of discrete, aqueous group 13 clusters. This report details the synthetic and structural characterization of these compounds, which are of interest as precursors (inks) for thin-film oxides with materials applications. Single-crystal X-ray diffraction (XRD) data show that the hexagonal unit cell lengths of these clusters fall within the range a, b = 20.134−20.694 Å and c = 18.266−18.490 Å. The unit cell volumes become larger (V = 6494−6774 A^3) with increasing indium occupancy. The compositions of several Ga/In clusters determined by electron probe microanalysis and elemental analysis are in agreement with single-crystal XRD results. The transformation of the Ga/In clusters to metal oxides at high temperature was studied using variable-temperature powder XRD. With heating, the Ga/In clusters with lower indium occupancies convert to the β-Ga_2O_3 structure. For clusters with higher indium occupancies, phase separation occurs, and an In_2O_3 bixbyite-type structure forms. The stoichiometric control at the molecular level demonstrated herein is important in designing functional thin films of metal oxides due to the tunable nature of these heterometallic solution precursors. In addition, information about the solid-state structure of these compounds leads to a fundamental understanding of the materials properties of these clusters for future thin-film and precursor development.

INTRODUCTION

The group 13 metals, specifically aluminum, gallium, and indium, exhibit unique hydrolytic and condensation behavior in solution as a dynamic, pH-dependent series of structures that range from hydrated monomers to bridged hydroxide oligomers to oxides.[1−12] For decades cationic aluminum cluster species have received attention because of their environmental importance as flocculants and coagulants, for the transport of heavy metals, as well as their toxicity to plants and aquatic organisms.[13−19] Corresponding nanoscale gallium clusters have received less attention, although several discrete group 13 metal hydroxo/aquo structures have been successfully isolated and structurally characterized.[5,7,10,20] The hydrolysis products of three different starting metal salts that produce ***f*-Ga_{13}**,[20] ***f*-Al_{13}**,[9] and the heterometallic ***f*-Ga_7In_6**[10] were previously reported and are designated by the symbol *f* (aka, flat) to differentiate them from the more widely studied Al_{13} Keggin (**κ-Al_{13}**) structures.[8,21−24] For the remainder of this manuscript a specific "flat" cluster identified by its metal content, for example, $Ga_{13}(\mu_3\text{-OH})_6(\mu\text{-OH})_{18}(H_2O)_{24}(NO_3)_{15}$, will be referred to as ***f*-Ga_{13}**.[25]

Most preparations of group 13 hydroxide structures have utilized organic supporting ligands to form stable clusters through charge balance and controlled hydrolysis.[5,25−29] For example, aminocarboxylate ligands such as *N*-(2-hydroxyethyl)-iminodiacetic acid (H_3heidi) have been used to synthesize ligand-supported versions of ***f*-Al_{13}** and ***f*-Ga_{13}**, as well as **Ga_2** and **Ga_8** intermediates.[4,25,30,31] While many procedures exist to prepare such compounds, they do not enable large structural diversity owing to the aforementioned interplay of pH and charge balance; the isolation of only a few different structure types has occurred. As a result, a general synthetic strategy with a multitude of outputs is highly desirable. Furthermore, organic supporting ligands can lead to defects and impurities when these clusters are used as materials precursors (inks), thus limiting their utility for bulk and thin-film oxides.

Until recently group 13 heterometallic **$(M,M')_{13}$** clusters have been notably absent in the families of ligand-supported and purely inorganic **M_{13}** structures. The ***f*-Ga_7In_6** cluster, which was the first example of such an inorganic structure type, proved to be an effective single-source precursor for the preparation of a high-quality dense, smooth, and amorphous IGO thin film with a reported $In_{0.92}Ga_{1.08}O_3$ composition.[10] ***f*-Ga_7In_6** (in similar fashion to the previously reported ***f*-Ga_{13}** cluster) was synthesized by dissolving metal nitrate salts in methanol with an organic nitroso compound as an additive. Partial evaporation of these solutions at room temperature and open to air produced crystals within two weeks. Under slightly basic conditions (requiring the addition of NaOH, NH_4OH, or

Received: January 15, 2015
Published: April 1, 2015

DOI: 10.1021/acs.inorgchem.5b00097
Inorg. Chem. 2015, 54, 3913−3920

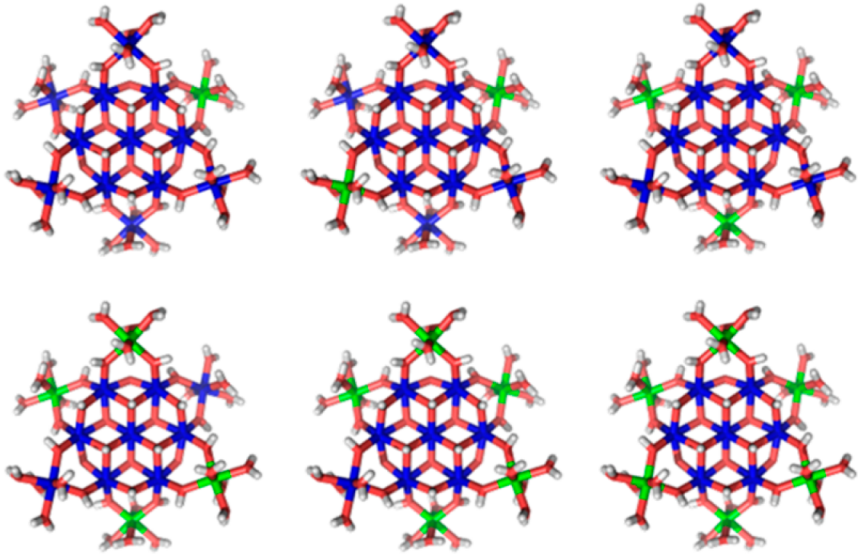

Figure 1. *f*-$Ga_{13-x}In_x$ (x = 1−6) heterometallic hydroxo-aquo clusters. Clockwise from the top right: $Ga_{12}In_1$ (**1**), $Ga_{11}In_2$ (**2**), $Ga_{10}In_3$, (**3**), Ga_9In_4 (**4**), Ga_8In_5 (**5**), and Ga_7In_6 (**6**). Gallium and indium metal ions are colored in blue and green, respectively. All six Ga/In positions in the outer ring are symmetrically equivalent. The X-ray structures show that the seven interior positions in each cluster are occupied by only Ga ions, and the gallium and indium ions in the outer ring are disordered over all six positions rather than in specific locations.

$Al(OH)_3$), hydrated $Al(NO_3)_3$ forms the related *f*-Al_{13} cluster with coprecipitation of other products.[9]

As an extension to this previous work, a series of heterometallic *f*-$Ga_{13-x}In_x$ (x = 1−6) hydroxide structures (**1**−**6**) is now presented (Figure 1). Published synthetic and structural details for *f*-Ga_7In_6 are included for comparison with the new heterometallic Ga/In clusters. This synthesis provides facile tuning of the Ga/In ratio at the molecular level, providing a means by which to alter of the properties of metal oxide thin films fabricated from these precursors.

EXPERIMENTAL SECTION

General Methods. All reagents were purchased from commercial sources and used as received. Gallium nitrate hydrate (99.99% Ga) and indium nitrate hydrate (99.999% In) were purchased from Strem Chemicals. The organic additive *N*-nitrosodibutylamine (DBNA) was purchased from TCI America. Methanol (MeOH) was used as received. All reactions were conducted in standard 20 mL scintillation vials.

General Procedure for the Synthesis of *f*-$Ga_{13-x}In_x$ Clusters (1−6). $Ga(NO_3)_3$ and $In(NO_3)_3$ salt hydrates were dissolved in MeOH (10 mL). DBNA was added to this solution with a syringe; the solution was stirred uncapped and left undisturbed in air at room temperature. Within two weeks, most of the solvent evaporated, and colorless, block-shaped single crystals of **1**−**6** formed at the bottom of the vials. The product was isolated by removing the DBNA with a syringe and then washing the product crystals with acetone (yields ranging from 20 to 63%). The reagent ratios for clusters **1**−**6** are summarized in Table 1.

X-ray Crystallography. Single-crystal X-ray diffraction experiments were carried out on a Bruker Smart Apex diffractometer at 153 and 173 K using Mo Kα radiation (λ = 0.710 73 Å). Absorption corrections were applied by SADABS.[32] Details of data collection and structure refinement are given in Table 2.

Refinements of all crystal structures were performed in the same way. Disordered NO_3^- anions and solvent molecules were treated by SQUEEZE.[33] Corrections of the X-ray data by SQUEEZE provide a range of 591−679 electrons/cell, which bracket the required value of 621 electrons/cell for nine NO_3^- anions, 18 water molecules, and nine methanol molecules in the full unit cell. All non-hydrogen ions were refined with anisotropic thermal parameters. In all structures H ions were not taken into consideration. All calculations were performed using the Bruker SHELXTL package.[34]

Table 1. Ratios of $Ga(NO_3)_3$, $In(NO_3)_3$, and DBNA for the Clusters 1−6

structure	$Ga(NO_3)_3$[a] (g)	$In(NO_3)_3$ (g)	DBNA (mL)	yield
$Ga_{12}In_1$ (**1**)	0.250	0.059	0.8	20%
$Ga_{11}In_2$ (**2**)	0.072	0.042	0.6	33%
$Ga_{10}In_3$ (**3**)	0.250	0.252	0.6	62%
Ga_9In_4 (**4**)	0.050	0.118	0.2	63%
Ga_8In_5 (**5**)	0.050	0.323	0.4	35%
Ga_7In_6 (**6**)	0.050	0.588	0.7	23%

[a]The ratios of $In(NO_3)_3$ and DBNA are relative to the starting quantity of $Ga(NO_3)_3$.

Variable-Temperature Powder X-ray Diffraction. Powder XRD data were collected for all cluster compositions (*f*-Ga_{13} and **1**−**6**) on a Rigaku Ultima with a Cu Kα source (1.54 Å); 2θ = 5−60° at 0.5°/min. Ex situ heating was used to study the transformation from cluster to metal oxide. *f*-Ga_{13} was measured after heating to set temperatures of 250, 600, 800, 900, 1000, and 1100 °C for 4 h at a 10 °C per min ramp rate. Clusters **1**−**6** were heated in air as loose powders to the same temperatures as well as to 1200 °C under the same ramping conditions.[35] Topas Academic was used to perform Pawley fits to monitor changes to the phase and lattice parameters, and Rietveld refinements were performed to monitor the indium occupancy and to verify the coordination geometry.

Bulk Sample Analysis. Electron probe microanalysis (EPMA) measurements were carried out on a CAMECA SX50 Electron Microprobe. Desert Analytics conducted elemental analysis (EA) of bulk samples. *f*-Ga_7In_6 was prepared using a previously published method.[10,36]

RESULTS AND DISCUSSION

In early efforts to synthesize the series of *f*-$Ga_{13-x}In_x$ heterometallic clusters, the ratio of metal ions in the target compound was used to inform the starting ratio of $Ga(NO_3)_3$ to $In(NO_3)_3$. Single-crystal XRD data for the initial attempt to form *f*-Ga_7In_6 using a 7:6 ratio of $Ga(NO_3)_3$/$In(NO_3)_3$ revealed that *f*-$Ga_{10}In_3$ had formed instead. Subsequently, *f*-

DOI: 10.1021/acs.inorgchem.5b00097
Inorg. Chem. 2015, 54, 3913−3920

Table 2. Crystal Structure Data for Clusters 1−6 with Fractional Ion Values

	1	2	3	4	5	6
empirical formula	$C_6H_{96}Ga_{11.8}In_{1.2}N_{15}O_{99}$	$C_6H_{96}Ga_{10.27}In_{2.73}N_{15}O_{99}$	$C_6H_{96}Ga_{10.3}In_{2.7}N_{15}O_{99}$	$C_6H_{96}Ga_{9.1}In_{3.9}N_{15}O_{99}$	$C_6H_{96}Ga_{7.7}In_{5.3}N_{15}O_{99}$	$C_6H_{96}Ga_7In_6N_{15}O_{99}$
formula weight	2923.38	2992.46	2990.57	3045.14	3106.47	3139.94
crystal system	trigonal	trigonal	trigonal	trigonal	trigonal	trigonal
space group	$R\bar{3}$	$R\bar{3}$	$R\bar{3}$	$R\bar{3}$	$R\bar{3}$	$R\bar{3}$
temp, K	173 (2)	173 (2)	173 (2)	173 (2)	173 (2)	173 (2)
wavelength, Å	0.71073	0.71073	0.71073	0.71073	0.71073	0.71073
a, Å	20.1387(14)	20.2946 (12)	20.2925 (7)	20.4329(10)	20.6585(9)	20.6974(14)
b, Å	20.1387(14)	20.2946 (12)	20.2925 (7)	20.4329(10)	20.6585(9)	20.6974(14)
c, Å	18.490(3)	18.456(2)	18.4437 (12)	18.4080(18)	18.2996(8)	18.256(3)
α, deg	90	90	90	90	90	90
β, deg	90	90	90	90	90	90
γ, deg	120	120	120	120	120	120
V, Å^3	6494.3(11)	6583.2(9)	6577.3(5)	6655.8(8)	6763.5(5)	6773(1)
Z	3	3	3	3	3	3
calcd density, g cm^{-3}	2.242	2.264	2.265	2.279	2.288	2.310
abs coeff, mm^{-1}	4.08	3.96	3.96	3.86	3.74	3.704
F(000)	4361	44435	4441	4507	4580	4620
θ range, deg	2.5−28.2	2.5−28.2	2.5−28.2	2.5−28.2	2.5−28.0	2.5−27.0
refls collected/unique	13623/3412 [0.0317]	13370/3195 [0.0216]	13724/3464 [0.0217]	14035/3500 [0.0176]	15922/3642 [0.0560]	16375/3290 [0.0187]
refinement method	full matrix least-squares on F^2	full matrix least-squares on F^2	full matrix least-squares on F^2	full matrix least-squares on F^2	full matrix least-squares on F^2	full matrix least-squares on F^2
data/restraints/params	3412/0/166	3195/0/166	3464/0/166	3500/0/166	3642/0/166	3290/0/166
GOF on F^2	1.055	1.065	1.055	1.034	1.082	1.102
final *R* indices [$I > 2\sigma(I)$]	*R*1 = 0.0328, *wR*2 = 0.0886	*R*1 = 0.0257, *wR*2 = 0.0719	*R*1 = 0.0249, *wR*2 = 0.0709	*R*1 = 0.0237, *wR*2 = 0.0698	*R*1 = 0.0370, *wR*2 = 0.0961	*R*1 = 0.0246, *wR*2 = 0.0721
R indices (all data)	*R*1 = 0.0391, *wR*2 = 0.0916	*R*1 = 0.0282, *wR*2 = 0.0732	*R*1 = 0.0273, *wR*2 = 0.0719	*R*1 = 0.0253, *wR*2 = 0.0715	*R*1 = 0.0444, *wR*2 = 0.0997	*R*1 = 0.0256, *wR*2 = 0.0727
largest diff peak and hole, e Å^{-3}	1.064 and −0.373	0.858 and −0.312	0.845 and −0.353	0.864 and −0.352	0.990 and −0.989	1.034 and −0.406

DOI: 10.1021/acs.inorgchem.5b00097
Inorg. Chem. 2015, 54, 3913−3920

Ga_7In_6 was successfully prepared by using a 1:12 ratio of $Ga(NO_3)_3/In(NO_3)_3$ (a 1:10 ratio is also sufficient, as shown in Table 1).[10] The excess of $In(NO_3)_3$ required to produce the desired product suggested a solubility of $In(NO_3)_3$ greater than that of $Ga(NO_3)_3$ in DBNA. A graph of the total Ga and In content in these two Ga/In heterometallic clusters and *f*-Ga_{13} versus the equivalents of $Ga(NO_3)_3$ and $In(NO_3)_3$ used provides a linear relationship that was then used as a guide to predict the ratio of starting materials required for the remaining Ga/In structures (Figure 2).

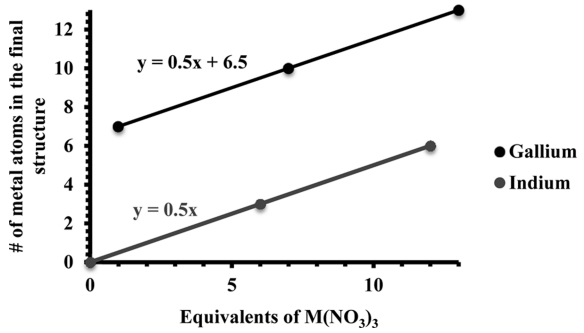

Figure 2. Plot of the relationships between the equivalents of $Ga(NO_3)_3$ and $In(NO_3)_3$ required to form *f*-$Ga_{13-x}In_x$ clusters and the number of gallium and indium ions in the final structure. The *y*-axis provides the number of corresponding metal ions in the final cluster. For example, to form *f*-$Ga_{10}In_3$, 7 equiv of $Ga(NO_3)_3$ must be used (value read for Ga = 10 on *y*-axis), while 6 equiv of $In(NO_3)_3$ are required (value read for In = 3 on *y*-axis).

This simplistic approach worked well, and the resulting starting ratios of $Ga(NO_3)_3$ and $In(NO_3)_3$ required to form *f*-$Ga_{12}In_1$, *f*-$Ga_{10}In_3$, *f*-Ga_9In_4, and *f*-Ga_8In_5 were found to be 5:1, 7:6, 1:2, and 2:11, respectively. The final Ga/In ratio for each cluster was determined by a single-crystal X-ray structure and refinement model with the Ga and In ions sharing the same positions in the outer shell of the cluster. EA and EPMA were used to confirm the metal ratios for bulk samples of several clusters with different indium substitutions (Table 3). The

Table 3. Metal ratios for 1, 3, 4, and 6 based on single crystal XRD, EA, and EPMA data. Standard deviations from EA and EPMA are shown in parentheses

	starting ratio Ga/In	XRD Ga/In	EA Ga/In	EPMA Ga/In
$Ga_{12}In_1$	5:1	12:1	11.75(0.02): 1.3(0.3)	11.8(0.1): 1.2(0.1)
$Ga_{10}In_3$	7:6	10:3	10.41(0.04): 2.6(0.1)	11.1(0.1): 2.0(0.1)
Ga_9In_4	1:2	9:4	8.921(0.009): 4.08(0.02)	9.5(0.1): 3.5(0.1)
Ga_7In_6	1:12	7:6	6.31(0.05): 6.69(0.04)	6.5(0.9): 6.5(0.9)

combination of both techniques resulted in metal ion ratios within error of those obtained from single-crystal XRD. A high degree of control over composition within heterometallic clusters has seldom been observed; thus, these clusters represent a simple way to control product ratios using the starting salt stoichiometry as the primary variable.[37]

Single-Crystal X-ray Structures of 1−6. Characterization of **1**−**6** by single-crystal XRD reveals structures similar to that of the previously reported *f*-Ga_{13} cluster.[20] Three different distorted octahedral metal coordination environments are observed in these compounds (core: **M1**, middle ring: **M2**, outer ring: **M3**; see Figure 3). All structures feature a rigid

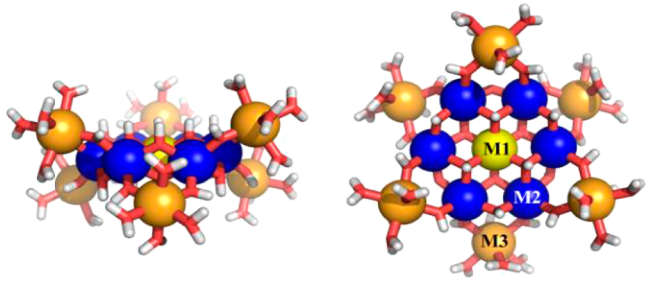

Figure 3. Side (left) and top (right) view of the three different coordination environments for the metal ion sites in **1**−**6**: **M1** (core, yellow), **M2** (middle, blue), and **M3** (outer, bronze).

planar core of seven gallium ions (**M1** and **M2**). The six outer ring metal ions (**M3**) are bound to the planar core by μ-OH bridges and alternate above and below the plane of said core; each outer ring metal ion fills its remaining coordination sites with four water molecules.

All compounds are isostructural and have a space group of symmetry $R\bar{3}$. All crystal structures are comprised of a $[(Ga_7)In_xGa_{6-x}(OH)_{18}(H_2O)_{24}]^{15+}$ (x = 0−6) cation located on a $\bar{3}$ axis. Three nitrate (NO_3^-) anions are in general positions; two form H-bonds with the $\mathbf{M_{13}}$ cation, while the third is disordered and shares six other possible positions around the cation with solvent molecules. Thus, the $\mathbf{M_{13}}$ cation in the crystal structure is surrounded by 15 NO_3^- anions and nine solvent molecules (three methanol and six water molecules) forming H-bonds with −OH groups and terminal water molecules bound to the metal ions in the outer ring. Solvent molecules sharing positions with the NO_3^- anion are disordered as well. All structures contain two nearby positions occupied by disordered solvent molecules (water or methanol) in a 1:1 ratio. In all clusters observed so far, refinements of occupation factors of the metal ions in the planar M_7 core are close to 1, meaning there is no disorder; therefore, only gallium ions occupy these positions. The observed Ga−O (1.926−1.963 Å) distances are typical for these bonds also indicating that gallium occupies all seven central core positions. The refined occupation factor of the metal ions in the outer ring of **1**−**6** is intermediate between that corresponding to gallium and indium ions. The M−OH and $M-OH_2$ distances found in the structures are in the range between the shorter Ga−O and longer In−O distances and depend on the Ga/In ratio for the metal ions in the outer ring. The unit cell volumes, which increase from 6494 Å^3 (*f*-Ga_{13}) to 6774 Å^3 (*f*-Ga_7In_6) help to approximate the level of substitution as more indium ions are incorporated into the outer ring of each structure.

The number of indium ions in the **M3** ring is determined by refinement of occupation factors for the gallium and indium ions sharing these positions. The refinement of occupation factors provides partial ion values for gallium and indium stoichiometries (e.g., *f*-$Ga_{10.3}In_{2.7}$ vs *f*-$Ga_{10}In_3$). All six Ga/In positions in the **M3** ring are symmetrically equivalent. The gallium and indium ions appear to be randomly distributed over the six positions, and their precise location in the clusters cannot be determined by modeling the single-crystal X-ray data. For example, there are three potential arrangements for **M3** indium ions in *f*-$Ga_{10}In_3$ (Figure 4).

DOI: 10.1021/acs.inorgchem.5b00097
Inorg. Chem. 2015, 54, 3913−3920

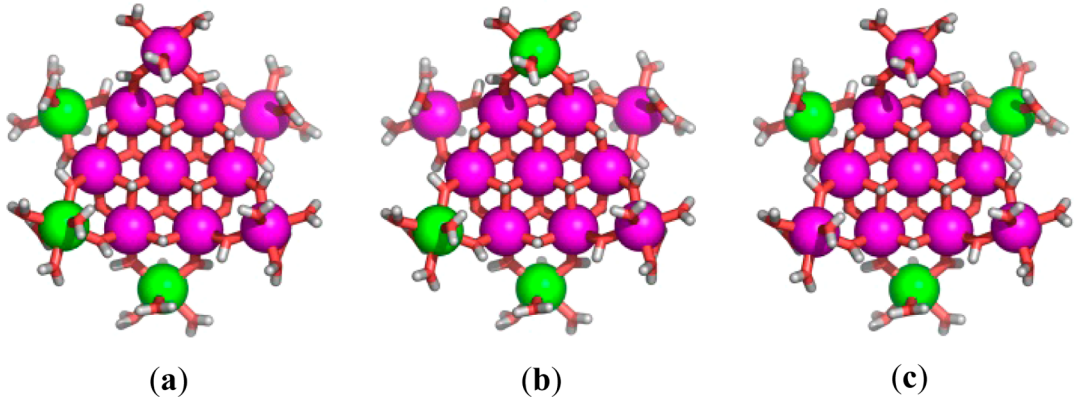

Figure 4. Potential arrangements of indium ions in the outer ring of *f*-$Ga_{10}In_3$.

Structure (**c**) in Figure 4 is the most reasonable arrangement; it is the most symmetric structure, and it affords the most space between indium ions (ionic radius (*r*): Ga = 62 pm, In = 80 pm).[38] In this case, the cluster would be rotationally disordered and result in a structure with partial value stoichiometries. It cannot be ruled out from single-crystal XRD that the observed single-crystal structures are mixtures of clusters with different stoichiometries (e.g., *f*-$Ga_{10}In_3$ = 50% *f*-Ga_7In_6 + 50% *f*-Ga_{13}) rather than a mixture of disordered heterometallic cluster isomers. It is important to note, however, that regardless of the makeup of the crystals according to crystallographic analysis, the ionic makeup of the final product can be tuned and confirmed by other methods. Furthermore, powder XRD data reported below suggest that all six heterometallic clusters are distinct species, and a recent complete structural solution of these clusters by ^{1}H NMR spectroscopy confirms that each cluster is a distinct species in wet DMSO and that all three isomers of, for example, *f*-$Ga_{10}In_3$ persist in solution.[39]

Conversion of Clusters to Oxides. One of the primary applications for these clusters is as precursor inks for the formation of oxide thin films. Experiments were performed to determine the types of oxides formed from the decomposition of these clusters with heating. Products were identified and compared to known gallium/indium oxides.[40,41] The dehydration of *f*-Ga_{13} produces a white amorphous solid that persists until 600 °C (Figure 5), at which point a reflection for nanocrystalline monoclinic gallium oxide (β-Ga_2O_3) emerges.

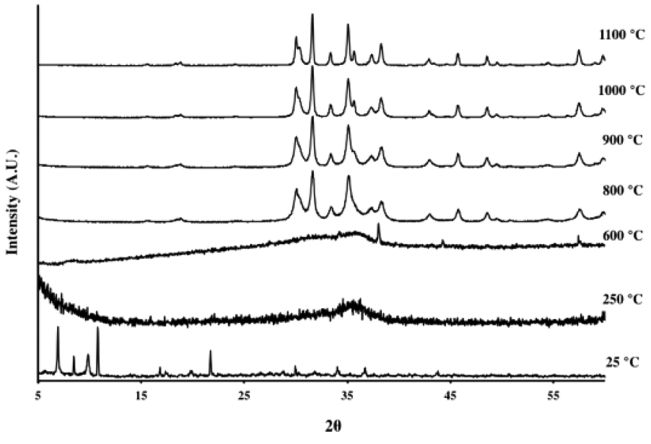

Figure 5. Powder XRD patterns for *f*-Ga_{13} cluster heated at specified temperatures.

Above 600 °C additional peaks appear and continue to sharpen as the temperature increases to 1100 °C.

At the other extreme, dehydration of *f*-Ga_7In_6 results in a primarily amorphous solid at much lower temperatures. Reflections for poorly ordered crystallites begin to emerge at temperatures as low as 250 °C. As with *f*-Ga_{13} more of these peaks arise above 600 °C and sharpen as the temperature increases to 1200 °C (Figure 6).

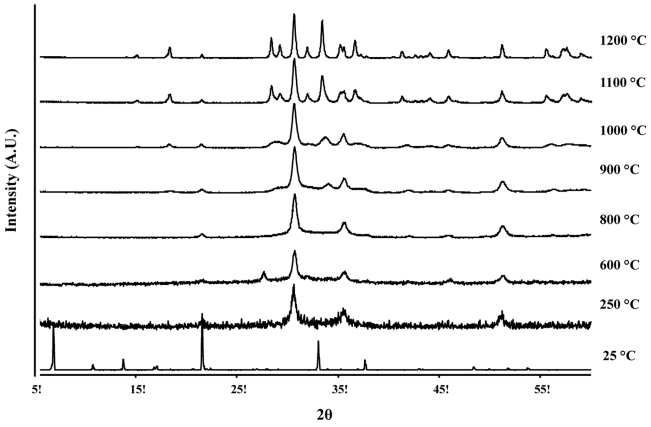

Figure 6. Powder XRD patterns for *f*-Ga_7In_6 cluster heated at specified temperatures.

The decomposition behaviors of **1**−**6** differ from what is observed for *f*-Ga_{13} (Figure 7). Broad reflections in **2**−**6** are

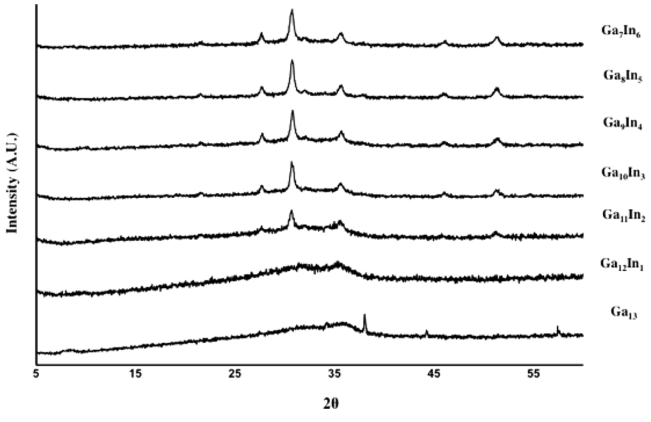

Figure 7. Powder XRD spectra of *f*-Ga_{13} and **1**−**6** at 600 °C.

DOI: 10.1021/acs.inorgchem.5b00097
Inorg. Chem. 2015, 54, 3913−3920

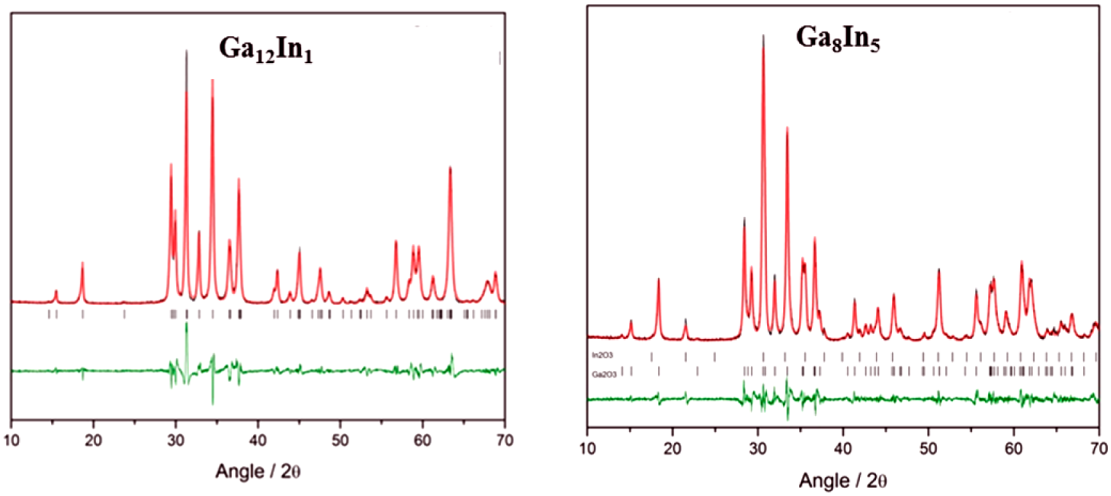

Figure 8. Pawley fits for *f*-$Ga_{12}In_1$ (**1**, left) and *f*-Ga_8In_5 (**5**, right). The observed trace (black), calculated trace (red), and the sum difference (green) are shown. **1** transforms into the *β*-Ga_2O_3 structure with elevated temperatures. Phase separation occurs for **5** at elevated temperatures and results in a majority phase of *β*-Ga_2O_3 and a minority phase of the In_2O_3 bixbyite-type structure.

Table 4. Lattice parameters of oxides formed from *f*-$Ga_{13-x}In_x$ clusters.

Ga_2O_3 parameters[a]—monoclinic				
	a/Å	*b*/Å	*c*/Å	*β*/deg
Ga_{13}	12.222(0.003)	3.042(0.001)	5.808(0.001)	103.88(0.01)
$Ga_{12}In_1$	12.455 (0.001)	3.1012(0.0003)	5.8662(0.0005)	103.444(0.006)
$Ga_{11}In_2$	12.581(0.003)	3.1207(0.0008)	5.916(0.002)	103.00(0.02)
$Ga_{10}In_3$	12.782(0.004)	3.1691(0.0007)	5.962(0.002)	102.48(0.02)
Ga_9In_4	12.803(0.002)	3.1805(0.0004)	5.9615(0.0009)	102.485(0.009)
Ga_8In_5	12.844(0.001)	3.1920(0.0001)	5.9757(0.0005)	102.401(0.008)
Ga_7In_6	12.8395(0.0007)	3.1928(0.0002)	5.9732(0.0007)	102.350(0.007)
In_2O_3 Parameters[a]—Cubic				
			a/Å	
Ga_8In_5			10.096(0.005)	
Ga_7In_6			10.0783(0.0004)	

[a]Standard deviations are shown in parentheses.

also visible at 600 °C, while ***f*-Ga_{13}** and ***f*-$Ga_{12}In_1$** are predominantly amorphous at this temperature. In fact, the heterometallic clusters (excluding ***f*-$Ga_{12}In_1$**) show reflections arising at lower temperatures than for ***f*-Ga_{13}** (see Supporting Information). Peaks for *β*-Ga_2O_3 begin to appear at 900 °C for all compounds, but the heterometallic clusters show a shift to smaller 2*θ* values relative to the standard *β*-Ga_2O_3 pattern due to the expansion of the lattice by the larger indium ions.

When heated, all compositions first transform into either a thermally robust amorphous oxide or a highly disordered nanocrystalline oxide. At higher temperatures **1**−**4** crystallize directly into a distorted *β*-Ga_2O_3 structure, while **5** and **6** phase separate upon crystallization into a majority phase of *β*-Ga_2O_3 and a minority phase of the bixbyite In_2O_3 structure as demonstrated in the Pawley fits for ***f*-$Ga_{12}In_1$** and ***f*-Ga_8In_5** (Figure 8). This mixed-phase composition arises once the *β*-Ga_2O_3 lattice stops expanding with increasing indium substitution (Table 4) and can therefore be thought of as occurring only after the gallium oxide lattice is completely saturated with indium.

These studies show that substitution of the larger indium ion results in an increase in the unit cell volume as well as the *a*, *b*, and *c* lattice parameters (confirmed by the powder XRD data) and a decrease in the *β* angles (Table 4). While Vegard's law applies only to solid solutions, a similar behavior is seen in these materials. The unit cell volume increases linearly as the amount of indium in the Ga_2O_3 lattic increases, until the point of indium saturation, where the unit cell volume levels off (Supporting Information, Figure S22). These changes can also be seen in the shift of *β*-Ga_2O_3 reflections as a function of indium content due to the substitution of indium for gallium into the lattice. As the In_2O_3 bixbyite structure emerges in the oxides formed from ***f*-Ga_8In_5** and ***f*-Ga_7In_6**, no significant peak shifts are observed in the *β*-Ga_2O_3 phase above $x = 0.62$ suggesting this system has an indium saturation limit between $x = 0.62$ (32 mol %) and $x = 0.77$ (38 mol %). This value is lower than that reported by Edwards et al. (42 mol %),[42] but falls within the range reported by Shannon and Prewitt (33−50 mol %).[43] Indium incorporation into the *β*-Ga_2O_3 structure has been previously studied showing preferential substitution of indium into octahedral gallium sites to form the *β*-$GaInO_3$ structure.[42,43] This result was also confirmed through Rietveld refinements of ***f*-Ga_{13}** and **1**−**6**, with a variable occupancy parameter assigning 100% of the indium ions to octahedral vacancies (see representative Rietveld refinement in Supporting Information).

DOI: 10.1021/acs.inorgchem.5b00097
Inorg. Chem. 2015, 54, 3913−3920

CONCLUSION

Synthetic control over the metal ratios in a series of heterometallic group 13 tridecameric hydroxo−aquo clusters (from *f*-$Ga_{12}In_1$ to *f*-Ga_7In_6) has been demonstrated. The variability of this synthesis enables highly specific molecular control over the composition of bulk metal oxides as well. Powder XRD studies show that heat treatment of *f*-Ga_{13} and the heterometallic clusters leads to different metal oxide structures depending on the fraction of indium within the cluster. These studies also provide a saturation limit for incorporation of indium into the final β-Ga_2O_3-type phase.

These heterometallic clusters represent a new set of compounds with implications in the development of single-source precursor inks for the fabrication of metal oxide thin films. The preparation of these clusters could enable the isolation of new heterometallic clusters that include non-group 13 metals as well. Stability of the planar M_7 core suggests the outer ring metal ions are components amenable to trans-metalation.[44] These compounds lead to a promising pathway for a new subset of heterometallic materials.

ASSOCIATED CONTENT

Supporting Information

CIF files of crystallography data for structures **1**−**6** in this work, variable-temperature powder XRD data of all clusters, Pawley fits for **1**−**6**, representative Rietveld refinement of $Ga_{12}In_1$. This material is available free of charge via the Internet at http://pubs.acs.org.

AUTHOR INFORMATION

Corresponding Authors

*E-mail: dwj@uoregon.edu. URL: http://sustainablematerialschemistry.org/. (D.W.J.)

*E-mail: Michelle.Dolgos@oregonstate.edu. (M.R.D.)

Present Address

⊥Division of Science and Mathematics, University of Minnesota Morris, Morris, MN 56267.

Notes

The authors declare no competing financial interest.

ACKNOWLEDGMENTS

We gratefully acknowledge the NSF Center for Sustainable Materials Chemistry (CHE-1102637) and a previous NSF Integrative Graduate Education and Research Traineeship (M.K.K.-D.; DGE-0549503) for generous financial support. D.W.J. is a Scialog Fellow of Research Corporation for Science Advancement and gratefully acknowledges additional support provided to assist this project.

REFERENCES

(1) Baes, C. F.; Mesmer, R. E. *The Hydrolysis of Metal Cations;* Wiley: New York, 1976.

(2) Zhong, S.; Zhao, H. D.; Tong, H. G. E.; Wang, R. F.; Zhu, F. Z. *Chin. J. Struct. Chem.* **2006**, *25*, 1217−1227.

(3) Casey, W. H.; Phillips, B. L.; Furrer, G. *Rev. Mineral. Geochem.* **2001**, *44*, 167−190.

(4) Schmitt, W.; Jordan, P. A.; Henderson, R. K.; Moore, G. R.; Anson, C. E.; Powell, A. K. *Coord. Chem. Rev.* **2002**, *228*, 115−126.

(5) Goodwin, J. C.; Teat, S. J.; Heath, S. L. *Angew. Chem., Int. Ed.* **2004**, *43*, 4037−4041.

(6) Casey, W. H.; Olmstead, M. M.; Phillips, B. L. *Inorg. Chem.* **2005**, *44*, 4888.

(7) Gerasko, O. A.; Mainicheva, E. A.; Naumov, D. Y.; Kuratieva, N. V.; Sokolov, M. N.; Fedin, V. P. *Inorg. Chem.* **2005**, *44*, 4133.

(8) Casey, W. H. *Chem. Rev.* **2006**, *106*, 1−16.

(9) (a) Gatlin, J. T.; Mensinger, Z. L.; Zakharov, L. N.; MacInnes, D.; Johnson, D. W. *Inorg. Chem.* **2008**, *47*, 1267−1269. (b) Wang, W.; Wentz, K. M.; Hayes, S. E.; Johnson, D. W.; Keszler, D. A. *Inorg. Chem.* **2011**, *50*, 4683.

(10) Mensinger, Z. L.; Gatlin, J. T.; Meyers, S. T.; Zakharov, L. N.; Keszler, D. A.; Johnson, D. W. *Angew. Chem., Int. Ed.* **2008**, *47*, 9484−9486.

(11) Mensinger, Z. L.; Zakharov, L. N.; Johnson, D. W. *Inorg. Chem.* **2009**, *48*, 3505−3507.

(12) Swaddle, T. W.; Rosenqvist, J.; Yu, P.; Bylaska, E.; Phillips, B. L.; Casey, W. H. *Science* **2005**, *308*, 1450−1453.

(13) Seichter, W.; Mogel, H.-J.; Brand, P.; Salah, D. *Eur. J. Inorg. Chem.* **1998**, 795−797.

(14) Furrer, G.; Phillips, B. L.; Ulrich, K. U.; Pothig, R.; Casey, W. H. *Science* **2002**, *297*, 2245−2247.

(15) Gillberg, L.; Hansen, B.; Karlsoon, I.; Nordströmm, E. A.; Pålsson, A. *Kemira Kemwater* **2003**, 115−150.

(16) Duan, J.; Gregory, J. *Adv. Colloid Interface Sci.* **2003**, *100*−*102*, 475−502.

(17) Williams, R. J. P. *Coord. Chem. Rev.* **1996**, *149*, 1−9.

(18) Dietrich, D.; Schlatter, C. *Aquat. Toxicol.* **1989**, *3*, 197−212.

(19) Powell, A. K.; Heath, S. L. *Coord. Chem. Rev.* **1996**, *149*, 59−80.

(20) Rather, E.; Gatlin, J. T.; Nixon, P. G.; Tsukamoto, T.; Kravtsov, V.; Johnson, D. W. *J. Am. Chem. Soc.* **2005**, *127*, 3242−3243.

(21) Parker, W. O., Jr.; Millini, R.; Kiricsi, I. *Inorg. Chem.* **1997**, *36*, 571.

(22) Lee, A. P.; Furrer, G.; Casey, W. H. *J. Colloid Interface Sci.* **2002**, *250*, 269.

(23) (a) Johansson, G. *Acta Chem. Scand.* **1960**, *14*, 769−771. (b) Johansson, G. *Acta Chem. Scand.* **1960**, *14*, 771−773.

(24) Smart, S. E.; Vaughn, J.; Pappas, I.; Pan, L. *Chem. Commun.* **2013**, *49*, 11352−11354.

(25) Mensinger, Z. L.; Wang, W.; Keszler, K. A.; Johnson, D. W. *Chem. Soc. Rev.* **2012**, *41*, 1019−1030.

(26) Schmitt, W.; Baissa, E.; Mandel, A.; Anson, C. E.; Powell, A. K. *Angew. Chem., Int. Ed.* **2001**, *40*, 3578−3581.

(27) Jordan, P. A.; Clayden, N. J.; Heath, S. L.; Moore, G. R.; Powell, A. K.; Tapparo, A. *Coord. Chem. Rev.* **1996**, *149*, 281−309.

(28) Malone, S. A.; Cooper, P.; Heath, S. L. *Dalton Trans.* **2003**, 4572−4573.

(29) Mainicheva, E. A.; Gerasko, O. A.; Sheludyakova, L. A.; Naumov, D. Y.; Naumova, M. I.; Fedin, V. P. *Russ. Chem. Bull., Int. Ed.* **2006**, *55*, 267−275.

(30) Heath, S. L.; Jordan, P. A.; Johnson, I. D.; Moore, G. R.; Powell, A. K.; Helliwell, M. *J. Inorg. Biochem.* **1995**, *59*, 785−794.

(31) de la Caillerie, J. B. D.; Man, P. P.; Vicente, M. A.; Lambert, J. F. *J. Phys. Chem. B* **2002**, *106*, 4133−4138.

(32) Sheldrick, G. M. *SADABS;* University of Göttingen: Germany, 1995.

(33) Van der Sluis, P.; Spek, A. L. *Acta Crystallogr., Sect. A* **1990**, *A46*, 194−201.

(34) Bruker. *SMART, SAINT, and SHELXTL;* Bruker AXS Inc.: Madison, WI, 2000.

(35) Coelho, A. *Topas-Academic;* Coelho Software: Brisbane, Australia, 2012.

(36) Johnson, D. W.; Healey, E. R.; Gatlin, J. T.; Mensinger, Z. L. *Methods for Producing Gallium and Other Oxo/Hydroxo Metal Aquo Clusters*. U.S. Patent 7,927,569, Sept 7, 2006.

(37) For a related example of heterometallic clusters in which pH was used to alter final cluster stoichiometry, see: Cooper, G. J. T.; Newton, G. N.; Long, D.-L.; Kögerler, P.; Rosnes, M. H.; Keller, M.; Cronin, L. *Inorg. Chem.* **2009**, *48*, 1097−1104.

(38) Downs, A. J. *Chemistry of Aluminum, Gallium, Indium, and Thallium;* Blackie Academic & Professional: Glasgow, Scotland, 1993.

(39) Oliveri, A. F.; Wills, L. A.; Hazlett, C. R.; Carnes, M. E.; Cheong, P. H.-Y.; Johnson, D. W. *Manuscript submitted*. As an example, $Ga_{10}In_3$

DOI: 10.1021/acs.inorgchem.5b00097
Inorg. Chem. 2015, 54, 3913−3920

and $Ga_{11}In_2$ appear to be indistinguishable by single-crystal XRD: for multiple batches of these species, the Ga/In ratio is between 10:3 and 11:2. However, by ^1H NMR it is clear that these are distinct species.
(40) Geller, B. *J. Chem. Phys.* **1960**, *33*, 676−684 XRD powder patterns found using the Inorganic Crystal Structure Database (ICSD).
(41) Marezio, M. *Acta Crystallogr.* **1966**, *20*, 723−728 XRD powder patterns found using the ICSD.
(42) Edwards, D. D.; Folkins, P. E.; Mason, T. O. *J. Am. Ceram. Soc.* **1997**, *80*, 253−57.
(43) Shannon, R. D.; Prewitt, C. T. *J. Inorg. Nucl. Chem.* **1968**, *30*, 1389−1398.
(44) Kamunde-Devonish, M. K.; Jackson, M. N.; Mensinger, Z. L.; Zakharov, L. N.; Johnson, D. W. *Inorg. Chem.* **2014**, *53*, 7101−7105.

DOI: 10.1021/acs.inorgchem.5b00097
Inorg. Chem. 2015, 54, 3913−3920